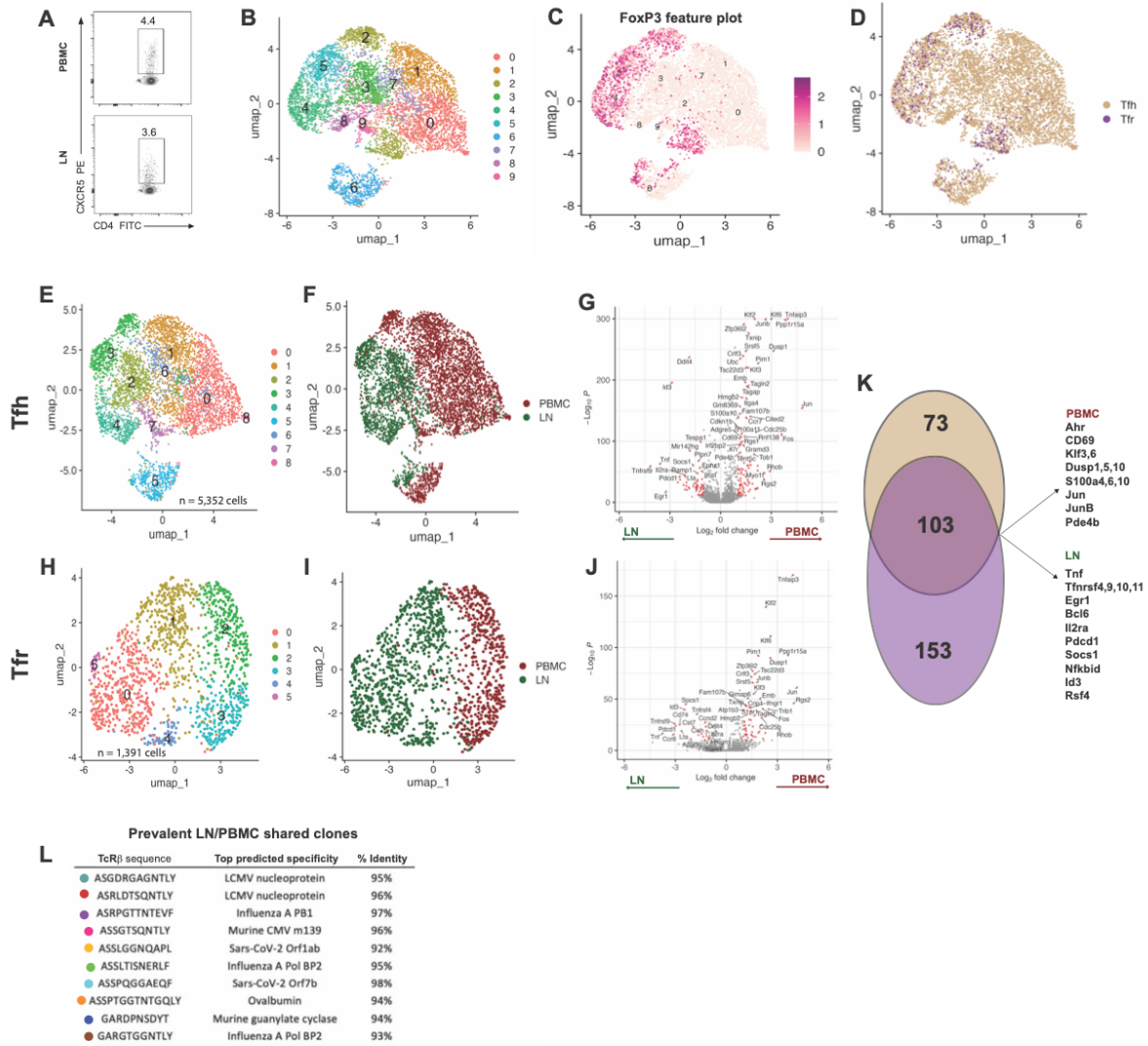
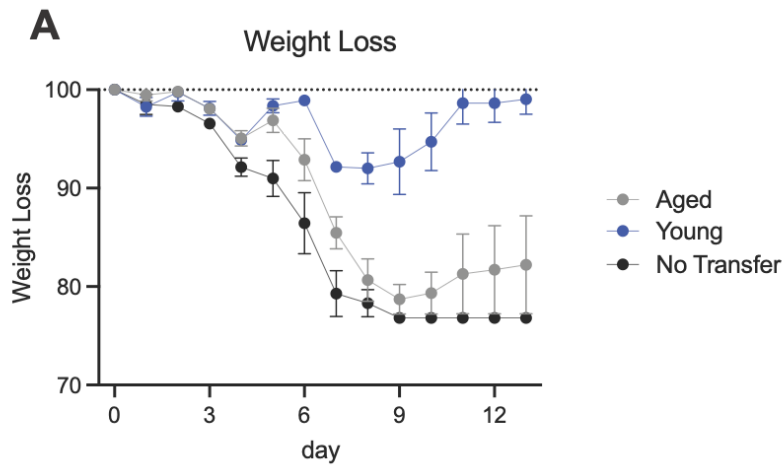


SUPPLEMENTAL MATERIAL

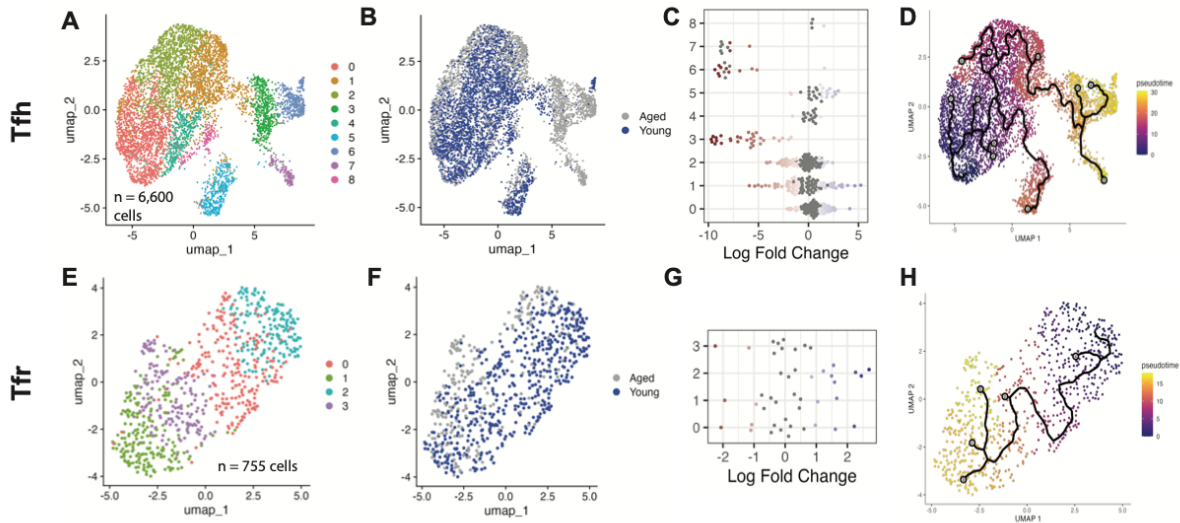


Supplemental Figure 1. Tfh and Tfr tissue-specific transcriptional profile after influenza vaccination.

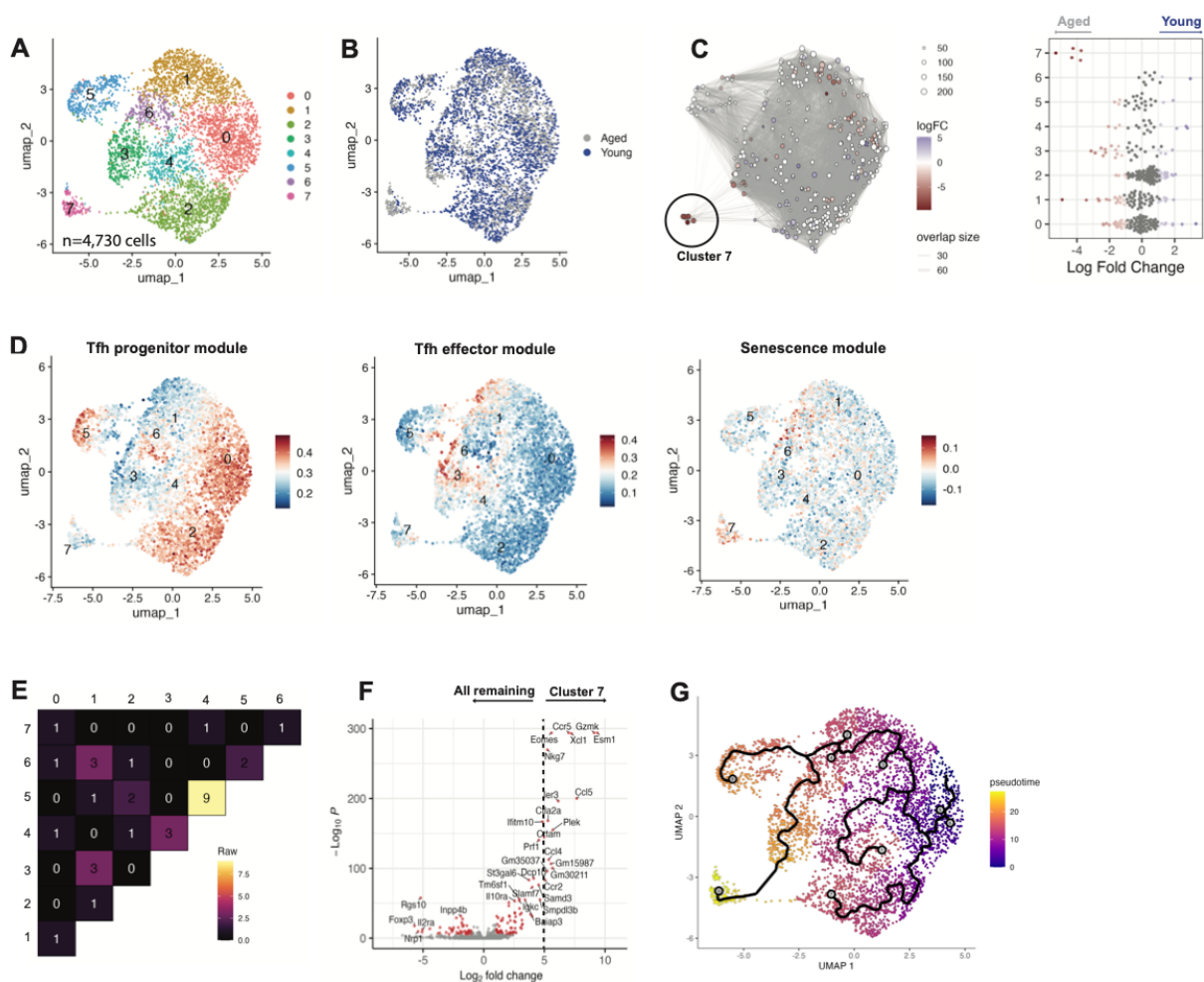
(A) Representative flow cytometry plots from CD4⁺CXCR5⁺ cell sorting, separated by tissue. Numbers denote CXCR5⁺ percentage of total CD4⁺ population. (B-D) UMAP projections of n=6,752 cells by unsupervised cluster assignment (B), FoxP3 feature plot (C), and by predicted cell type (assigned by SingleR) (D). (E and F) UMAP projection of n=5,352 Tfh cells alone with unsupervised clustering (E) and separated by tissue (F). (G) Volcano plot demonstrating differential gene expression (DEG) by tissue, with PBMC-enriched genes to the right of the y-axis and LN-enriched to the left. Red dots indicate genes meeting the significance threshold ($p < 10^{-10}$, fold change > 2). (H and I) UMAP projection of n = 1,391 Tfr cells alone with unsupervised clustering (H) and separated by tissue (I). (J) Volcano plot demonstrating DEGs by tissue, with PBMC-enriched genes to the right of the y-axis and LN-enriched to the left. Red dots indicate genes meeting the significance threshold ($p < 10^{-10}$, fold change > 2). (K) Venn diagram of PBMC vs. LN DEGs for Tfh (brown) and Tfr (purple). Select DEGs shared by Tfh and Tfr annotated to the right, separated by tissue. (L) TCR CDR3 amino acid sequence and top predicted specificity of the 10 most expanded clones shared between LN and blood Tfh. Data are from a single scRNAseq experiment of two individual mice concatenated.



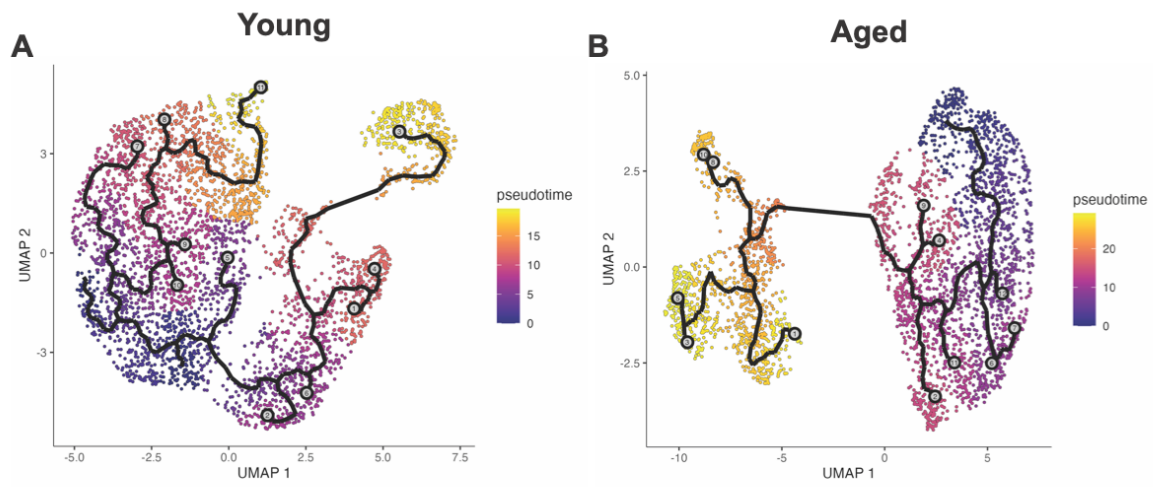
Supplemental Figure 2. Passive vaccination using serum from young, but not aged, mice is protective against severe influenza infection. Young mice were passively infused with 200ul serum from either aged or young inactivated H1N1(A/PR/8/34)/Addavax vaccinated donor mice (pooled from 3-4 mice). Recipients were challenged intranasally with 1LD₅₀ of PR8. Daily weights were obtained for 14 days following infection. n=3 young, n=4 aged. Data points represent the mean weight, and bars SEM.



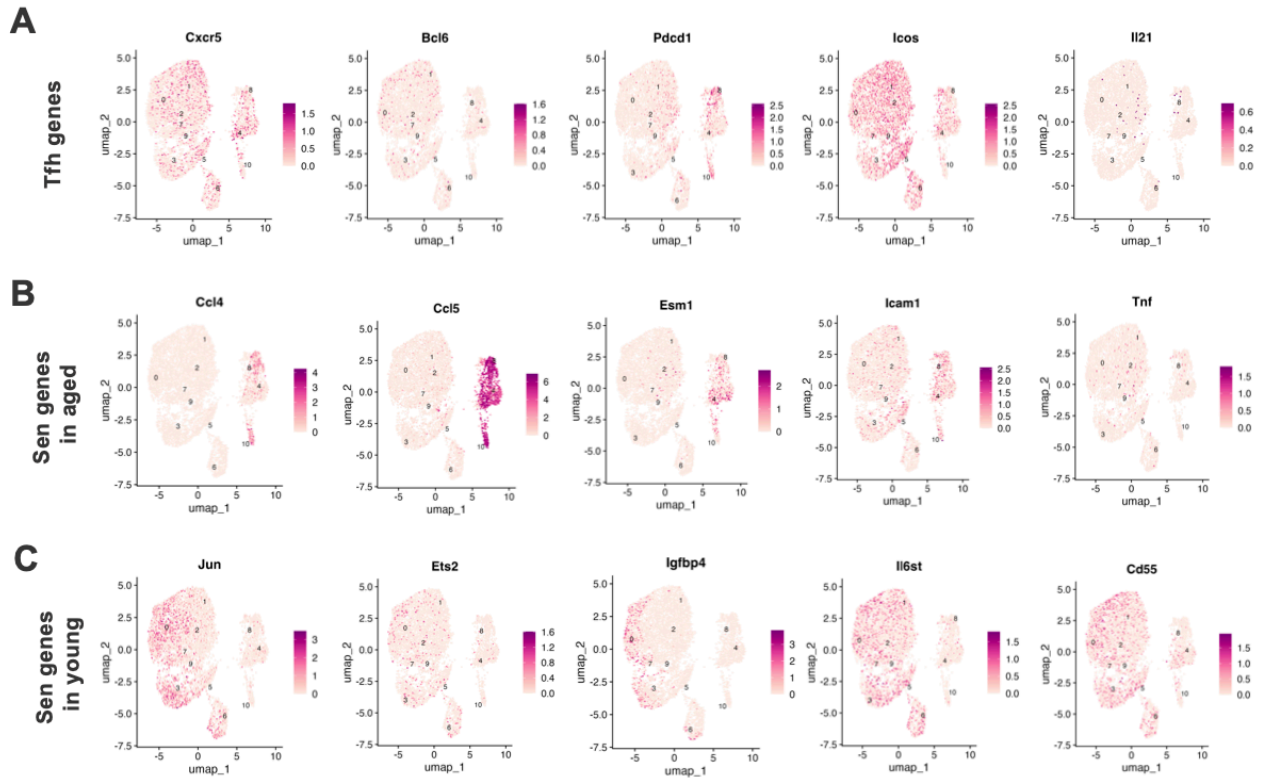
Supplemental Figure 3. Age-related transcriptional changes are more pronounced in cTfh cells than cTfr cells. (A and B) UMAP projections of n=6,600 young and aged cTfh by unsupervised cluster assignment (A) and age group (B). (C) MiloR cell neighborhood analysis illustrating differential abundance of cTfh cell neighborhoods in young (blue) versus aged (red) mice, represented by individual cluster (FDR<0.05, FC>2). (D) UMAP projection of cTfh Monocle3 pseudotime trajectories. (E and F) UMAP projections of n=755 young and aged cTfr by unsupervised cluster assignment (E) and age group (F). (G) MiloR cell neighborhood analysis illustrating differential abundance of cTfr cell neighborhoods in young versus aged mice, represented by individual cluster (FDR<0.05, FC>2). Data is concatenated data from two individual mice in each age group. (H) UMAP projection of cTfr Monocle3 pseudotime trajectories.



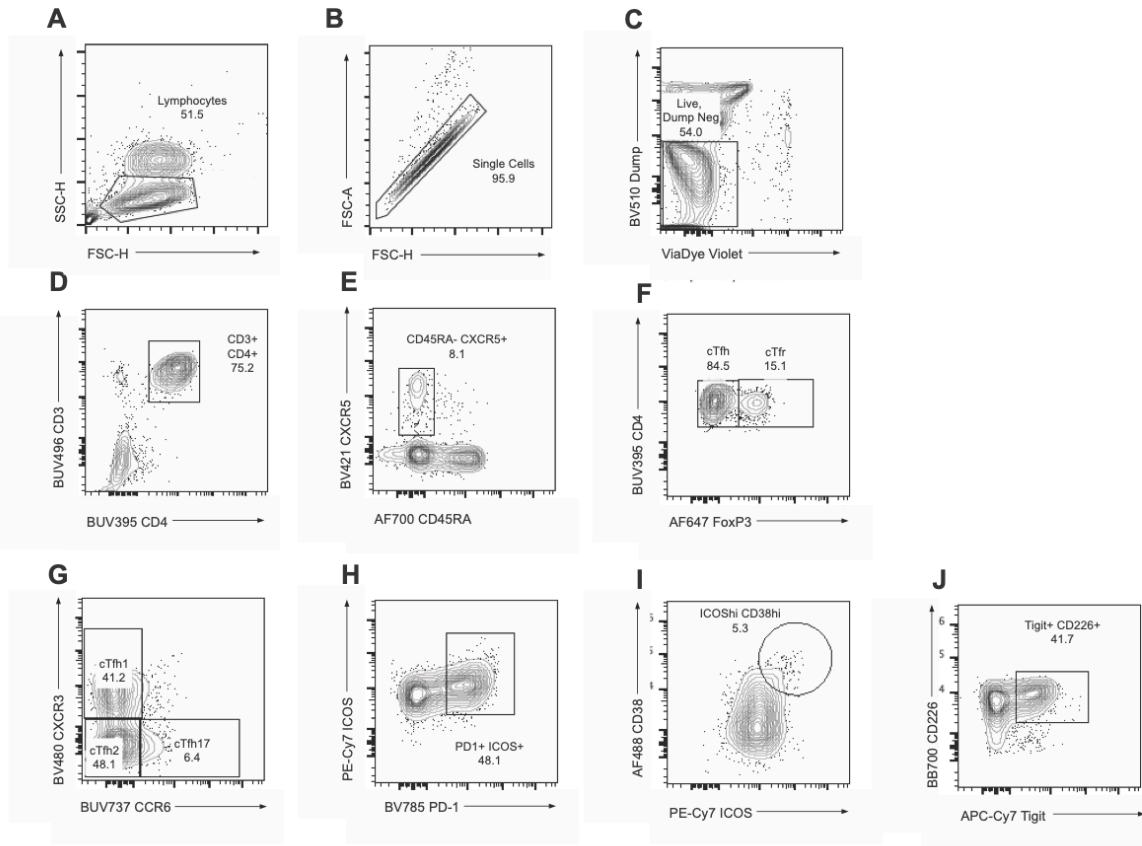
Supplemental Figure 4. Age-rewired Tfh cells with cellular senescence programs are also present in draining lymph node. (A and B) UMAP projections of n=4,730 young and aged lymph node follicular T cells by unsupervised cluster assignment **(A)** and age group **(B)**. **(C)** MiloR cell neighborhood analysis illustrating differential abundance of cell neighborhoods in young versus aged mice, represented in UMAP space or by individual cluster (FDR<0.05, FC>2). **(D)** Module score feature plots for a Tfh Progenitor module (14), Tfh Effector module (14), or a senescence module (29). **(E)** Clonal sharing (based on TCR sequence) including absolute number of shared clones between clusters. **(F)** Differentially expressed genes between cluster 7 and all remaining clusters. Red dots indicate ($p < 10^{-2}$, fold change > 2). **(G)** UMAP projection of lymph node follicular T cell Monocle3 pseudotime trajectories. Data is concatenated data from two individual mice in each age group.



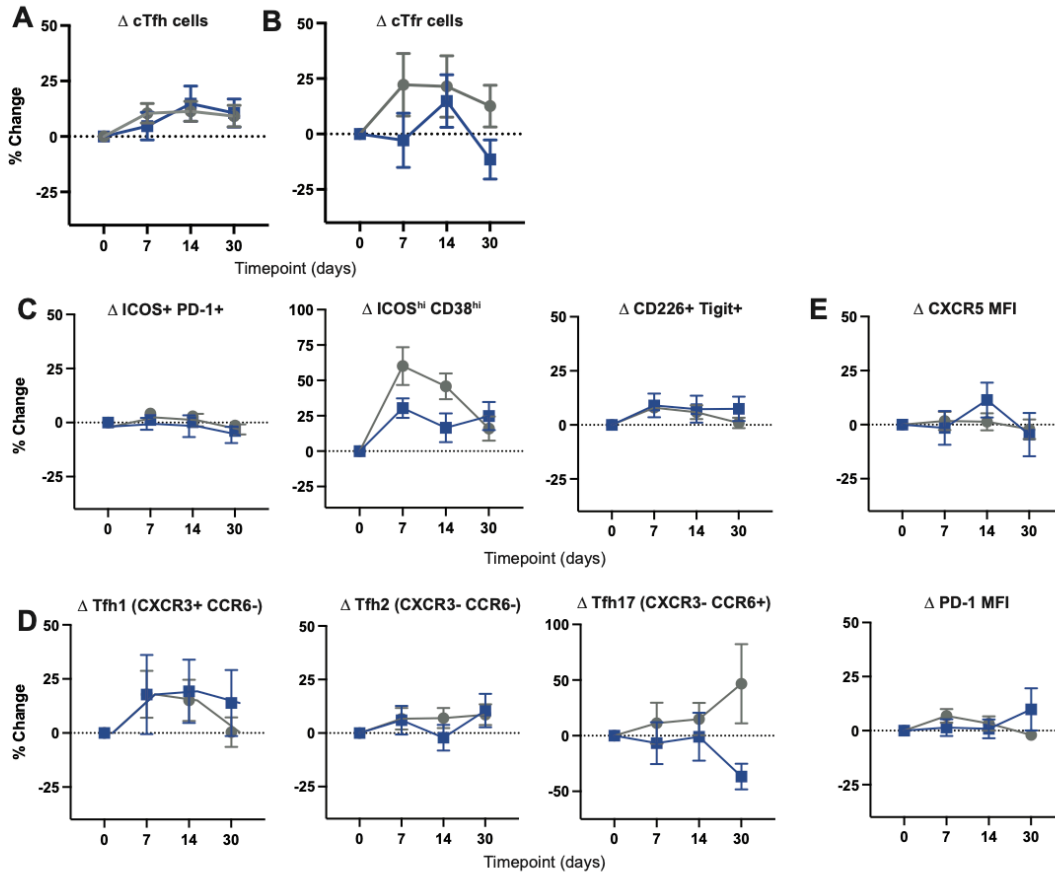
Supplemental Figure 5. Independent pseudotime analysis for young and aged mice. (A and B) UMAP projection of follicular T cell Monocle3 pseudotime trajectories for young (A) and aged vaccinated mice (B).



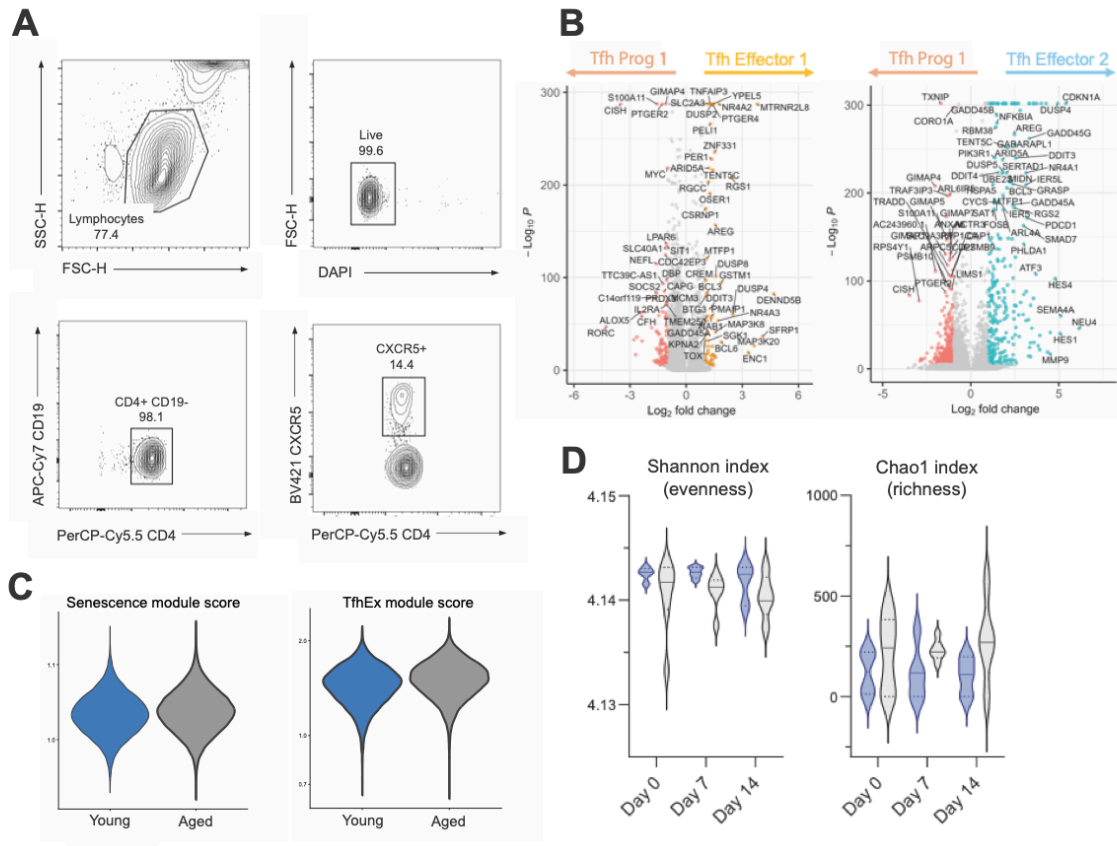
Supplemental Figure 6. Individual gene feature plots. (A-C) UMAP feature plot projections of $n=6,752$ cells denoting single gene expression for Tfh-associated genes (A), senescence-associated genes increased in aged cells (B), and senescence-associated genes increased in young cells (C).



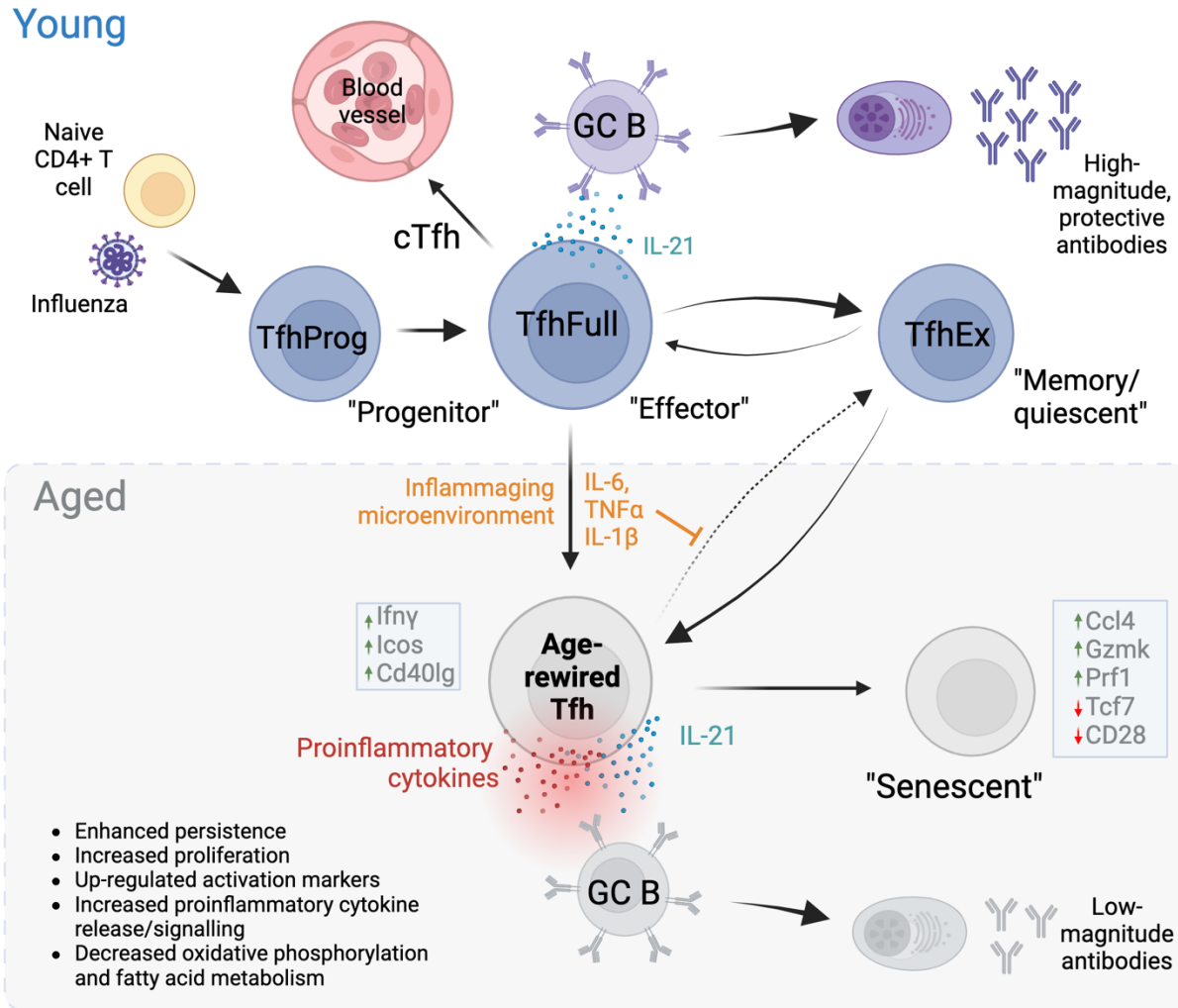
Supplemental Figure 7. High parameter spectral flow cytometry gating of follicular T cells. A lymphocyte gate was applied (A), then FSC singlets (B). Next, the live fraction of the “dump” negative ($CD8^- CD14^- CD19^-$) population was selected (C), and subsequently the $CD3^+ CD4^+$ subset identified (D). Follicular T cells were defined as $CD45RA^- CXCR5^+$ (E), then cTfh and cTfr subpopulations distinguished by FoxP3 staining (F). cTfh populations were further classified as $CXCR3^+ CCR6^-$ (cTfh1), $CXCR3^- CCR6^-$ (cTfh2), or $CXCR3^- CCR6^+$ (cTfh17) (G). Lastly, the fraction of cTfh co-expressing specific surface markers was defined including $PD1^+ ICOS^+$ (H), $CD38^+ ICOS^+$ (I), and $Tigit^+ CD226^+$ (J).



Supplemental Figure 8. Dynamic change of cTfh and cTfr populations after influenza vaccination. (A and B) Percent change from baseline (d0) of the cTfh frequency (A) and cTfr frequency (B) of total CD4⁺ T cells, separated by timepoint. (C) Percent change from baseline of specific Tfh subpopulations ICOS⁺PD1⁺ (left), ICOS^{hi}CD38^{hi} (middle), CD226⁺Tigit⁺ (right), separated by timepoint. (D) Percent change from baseline of different Tfh cell polarizations including Tfh1 (left), Tfh2 (middle), and Tfh17 (right) identified by indicated chemokine receptor expression. (E) Percent change from baseline CXCR5 (top) and PD1 (bottom) expression, measured as mean fluorescent intensity (MFI) by flow cytometry. All displayed data points represent mean value, with error bars indicating standard error. *p<0.05, uncorrected Mann-Whitney U test.



Supplemental Figure 9. Follicular T cell scRNAseq sorting strategy and additional analysis. (A) A lymphocyte gate was applied to CD4⁺-enriched PBMCs from young and aged influenza vaccinees (upper left), the live fraction identified (upper right), the CD4⁺ CD19⁻ populations selected (lower left), and the follicular T population identified by CXCR5 staining (lower right). **(B)** Volcano plots summarizing differential gene expression between cells in the Tfh Naïve 1 cluster and either Tfh Effector 1 (left) or Tfh Effector 2 (right) clusters ($p < 10^{-3}$, FC > 1). **(C)** Violin plots of overall module score for senescence (left) and the TfhEx developmental stage (right). **(D)** Shannon (left) and Chao1 (right) indexes representing Tfh cell clonal evenness and richness/diversity (respectively) in aged (gray) and young (blue) individuals at 0, 7, and 14 days following influenza vaccination.



Supplemental Figure 10. Graphical abstract. Naïve CD4+ T lymphocytes differentiate into Tfh progenitor (TfhProg) and subsequently Tfh effector (TfhFull) cells upon antigen stimulation (e.g. influenza vaccination). TfhFull cells secrete IL21 and interact with germinal center B cells, stimulating them to undergo class switch recombination, affinity maturation, and to differentiate into plasma cells. This effective stimulation results in the production of a high magnitude of protective antigen-specific antibodies. A subset of TfhFull enter the bloodstream and become circulating Tfh (cTfh). TfhFull can further differentiate into the TfhEx stage which exhibits a quiescent/memory phenotype. However, when stimulated by an inflammaging microenvironment, TfhFull cells are rewired. Importantly, age-rewired Tfh cells cannot transition to the TfhEx phenotype and can produce proinflammatory cytokines such as interferon γ in abundance. When age-rewired cells interact with GC B cells, there is less effective affinity maturation and plasma cell differentiation which results in a lower magnitude of antigen-specific antibodies. Furthermore, age-rewired Tfh can subsequently differentiate into senescent Tfh which exhibit a distinct proinflammatory transcriptomic profile.

Supplemental Table 1. Mouse scRNAseq absolute cell count by age and cluster.

| Cluster | Total Cells | Aged | | Young | |
|---------|-------------|---------|------|---------|------|
| | | # Cells | % | # Cells | % |
| 0 | 1340 | 450 | 33.6 | 890 | 66.4 |
| 1 | 1288 | 460 | 35.7 | 828 | 64.3 |
| 2 | 1218 | 660 | 54.2 | 558 | 45.8 |
| 3 | 697 | 158 | 22.7 | 539 | 77.3 |
| 4 | 642 | 563 | 87.7 | 79 | 12.3 |
| 5 | 515 | 175 | 34.0 | 340 | 66.0 |
| 6 | 504 | 153 | 30.4 | 351 | 69.6 |
| 7 | 445 | 173 | 38.9 | 272 | 61.1 |
| 8 | 384 | 341 | 88.8 | 43 | 11.2 |
| 9 | 175 | 53 | 30.3 | 122 | 69.7 |
| 10 | 152 | 151 | 99.3 | 1 | 0.7 |

Supplemental Table 2. Mouse scRNAseq senescence-associated gene differential expression.

| | Gene | log2 FC | Young exp | Aged exp | Adj P |
|-------------------|--------------------|---------|-----------|----------|-----------|
| Increased in aged | Ccl4 | -9.44 | 0 | 0.136 | 1.20E-123 |
| | Ccl3 | -7.06 | 0.001 | 0.093 | 5.21E-80 |
| | Ccl5 | -5.45 | 0.132 | 0.373 | 1.03E-159 |
| | Spp1 | -5.20 | 0 | 0.01 | 2.53E-05 |
| | Esm1 | -4.68 | 0.008 | 0.149 | 6.31E-116 |
| | Csf1 | -2.11 | 0.011 | 0.031 | 3.40E-05 |
| | Icam1 | -1.20 | 0.107 | 0.23 | 3.67E-42 |
| | Tnf | -1.07 | 0.018 | 0.036 | 0.028 |
| | Ptger2 | -0.85 | 0.069 | 0.11 | 2.88E-06 |
| | Increased in young | Pecam1 | 0.55 | 0.307 | 0.214 |
| Cd55 | | 0.69 | 0.247 | 0.153 | 3.80E-19 |
| Il6st | | 0.71 | 0.255 | 0.159 | 3.13E-19 |
| Igfbp4 | | 0.76 | 0.105 | 0.058 | 6.34E-09 |
| Ets2 | | 0.83 | 0.077 | 0.044 | 3.17E-05 |
| Jun | | 1.39 | 0.367 | 0.192 | 3.98E-63 |

Supplemental Table 3. Human cohort demographic characteristics

| | | Aged (n=78) | Young (n=18) |
|---------------------------|---|-------------|--------------|
| Median age (range) | | 69 (65-84) | 26 (19-38) |
| Sex - number (%) | Male | 17 (31) | 8 (44) |
| | Female | 37 (69) | 9 (56) |
| Vaccine type - number (%) | Standard | 4 (7) | 14 (88) |
| | High dose | 42 (78) | 0 (0) |
| | Unknown | 8 (15) | 2 (12) |
| Race - number (%) | White | 50 (93) | 10 (63) |
| | Black | 0 (0) | 2 (13) |
| | American Indian or Alaska Native | 0 (0) | 1 (6) |
| | Native Hawaiian or other Pacific Islander | 0 (0) | 0 (0) |
| | Asian | 2 (4) | 0 (0) |
| | Other, or more than one race | 0 (0) | 3 (19) |
| | Decline to answer | 2 (4) | 0 (0) |
| Ethnicity - number (%) | Hispanic or Latino | 0 (0) | 0 (0) |
| | Not Hispanic or Latino | 43 (80) | 15 (94) |
| | Decline to answer | 11 (20) | 1 (6) |

Supplemental Table 4. Median HAI titer and MSD binding, separated by age group.

| Timepoint | Aged H1 HAI titer | | | Young H1 HAI titer | | | Aged H1 Binding MSD | | | Young H1 Binding MSD | | |
|-----------|-------------------|--------|-------|--------------------|--------|-------|---------------------|--------|-------|----------------------|--------|-------|
| | Male | Female | P* | Male | Female | P* | Male | Female | P* | Male | Female | P* |
| 0 | 40 | 40 | 0.917 | 160 | 40 | 0.793 | 12461 | 29105 | 0.060 | 33987 | 26579 | 0.566 |
| 7 | 40 | 80 | 0.429 | 320 | 40 | 0.568 | 25115 | 30667 | 0.289 | 41472 | 34194 | 0.566 |
| 14 | 80 | 80 | 0.526 | 320 | 160 | 0.632 | 28117 | 50782 | 0.128 | 53919 | 43331 | 0.646 |
| 30 | 80 | 80 | 0.535 | 320 | 160 | 0.565 | 20265 | 34734 | 0.128 | 42279 | 34658 | 0.574 |

*Mann-Whitney U test, with Bonferroni p-value correction